A source of extended HCO$^+$ emission in young stellar objects

J. M. C. Rawlings,* S. D. Taylor and D. A. Williams
Department of Physics and Astronomy, University College London, Gower Street, London WC1E 6BT

ABSTRACT

Anomalous molecular line profile shapes are the strongest indicators of the presence of the infall of gas that is associated with star formation. Such profiles are seen for well-known tracers, such as HCO$^+$, CS and H$_2$CO. In certain cases, optically thick emission lines with appropriate excitation criteria may possess the asymmetric double-peaked profiles that are characteristic of infall. However, recent interpretations of the HCO$^+$ infall profile observed towards the protostellar infall candidate B335 have revealed a significant discrepancy between the inferred overall column density of the molecule and that which is predicted by standard dark cloud chemical modelling.

This paper presents a model for the source of the HCO$^+$ emission excess. Observations have shown that, in low-mass star-forming regions, the collapse process is invariably accompanied by the presence of collimated outflows; we therefore propose the presence of an interface region around the outflow in which the chemistry is enriched by the action of jets. This hypothesis suggests that the line profiles of HCO$^+$, as well as other molecular species, may require a more complex interpretation than can be provided by simple, chemically quiescent, spherically symmetric infall models.

The enhancement of HCO$^+$ depends primarily on the presence of a shock-generated radiation field in the interface. Plausible estimates of the radiation intensity imply molecular abundances that are consistent with those observed. Further, high-resolution observations of an infall-outflow source show HCO$^+$ emission morphology that is consistent with that predicted by this model.

Key words: stars: formation – ISM: clouds – ISM: jets and outflows – ISM: molecules.

1 INTRODUCTION

Within molecular clouds there exist 'cores' of denser material (with number densities of hydrogen nuclei, $n_H \gtrsim 10^4 \, \text{cm}^{-3}$). If these cores are gravitationally supercritical, gravitational collapse may occur, resulting in the formation of a protostar. The detection of the associated infall of gas has been the aim of many studies in recent years, by way of the distinctive line profiles of molecular species that trace appropriate density regions. If the lines are optically thick and the infall regions can be approximated by a spherically symmetric collapse with negative temperature and velocity gradients, then simple considerations (e.g. Rawlings 1996) show that the line profiles are expected to be double-peaked with the 'blue' wing stronger than the 'red' wing. Optically thin lines (originating from higher level transitions) of the same species are expected to be broader, with no self-reversal. Such profiles are seen in several protostar candidate sources for well-known tracers, such as CS, H$_2$CO, NH$_3$ and HCO$^+$ (e.g. Walker et al. 1986; Gregersen et al. 1997). However, the interpretation of

these profiles is critically dependent on the assumptions that are made concerning the collapse dynamics (e.g. Rawlings, Evans & Zhou 1993) and the spatial structure of the chemical abundances (Rawlings & Yates, in preparation).

HCO$^+$ is a particularly interesting species in that it is one of the few molecular ions to be detected in dark clouds. It is also one of the most widely used infall tracers (typically through observations of the $J = 3 \rightarrow 2$ and $4 \rightarrow 3$ transitions; see Gregersen et al. 1997 for a review of recent observations). The chemical significance of HCO$^+$ is confirmed by models which predict it to be the most abundant molecular ion in dark molecular clouds (e.g. Dalgarno & Lepp 1984). In fact, in the innermost (darkest, densest) regions of a molecular core these models suggest that HCO$^+$ may be the dominant ionized species (atomic or molecular), and as such it gives a measure of the total ionization level.

The Class 0 protostellar source B335 is currently the best known example of a potential infall source, in that it demonstrates all of the expected line-profile shapes as described above, and appears to be approximately spherical. It is reasonably close, and has a well-defined physical and kinematic structure (e.g. Zhou et al. 1993, 1994; Choi et al. 1995). However, several recent

* E-mail: jcr@star.ucl.ac.uk

observations of the HCO^+ profiles towards B335 have identified a puzzling anomaly: if the assumptions of a spherically symmetric radial inflow are correct, then radiative transfer modelling of the line profiles suggest that the HCO^+ fractional abundance (by number, relative to hydrogen nuclei) may be as high as 4×10^{-8}. The line profiles have been modelled with several radiative transfer codes, including a lambda iteration technique (STENHOLM; H. Buckley, private communication), a more sophisticated accelerated lambda iteration model which specifically caters for optically thick lines (SMMOL; Rawlings & Yates, in preparation) and Monte Carlo methods (Choi et al. 1995). Although there are some fundamental differences between these models, none of which can be regarded as perfect, they all require the fractional abundance of the HCO^+ to be *at least* an order of magnitude greater than that which can be accounted for either by chemical models of cold ($T \sim 10$ K) quiescent clouds or by more complicated models of the chemistry in dynamically evolving (isothermal) protostellar cores (Rawlings et al. 1992). The scale of this anomaly depends on the particular radiative transfer model of the observed line profile that is used for comparison, but in any event there does not seem to be any simple way of explaining the HCO^+ overabundance by reference to simple gas-phase or even gas–grain chemistries in idealized isothermal infall models. For the purpose of reference we will compare our model results to the abundances that are suggested by both the SMMOL and the Monte Carlo radiative transfer models when coupled to the simple 'inside-out' hydrodynamical collapse model of Shu (1977). The best fit in these models is obtained with an HCO^+ fractional abundance of 3.5×10^{-8} within the infalling region ($r \leq 0.03$ pc), where the mean density of the line-forming region is of the order of 10^4 cm^{-3}, and 3.5×10^{-9} in the surrounding static envelope (N. J. Evans, private communication). For comparison, models of quiescent dark clouds (with density 10^4 cm^{-3}, and temperature 10 K) predict a value of $\sim 3 \times 10^{-9}$ (van Dishoeck 1998). Of course, this value is dependent on the assumed values of the density and the cosmic ray ionization rate (ζ). However, the density is reasonably well constrained by the radiative transfer models and ionization studies (e.g. Williams et al. 1998). ζ is less well constrained, but Williams et al. suggest that a value of 5×10^{-17} s^{-1} is consistent with the ionization balance. This is not very different from the rate of 1.3×10^{-17} s^{-1} that is assumed in 'standard' models of dark clouds. In any case, since B335 is an isolated globule, there is little reason to suggest that ζ is anomalously high.

In the following section we present a model for the production of an HCO^+ excess. In this model, the chemistry is driven by localized heating. The heating is powered by the dynamical interaction of high-energy outflows that accompany protostellar inflow.

2 THE HYPOTHESIS AND MODEL

Observations have clearly shown that protostellar collapse is usually accompanied by the presence of collimated outflows (e.g. Bachiller et al. 1995). This naturally leads to some confusion in the interpretation of the observed line profiles. If, as is usually the case, the tracer molecule is present in both the infall and outflow components, it is necessary to disentangle the various velocity components. The molecules may be formed chemically in the outflow, or may exist simply by virtue of being present in the swept-up ambient gas. It was also shown in previous papers (Taylor & Williams 1996, hereafter Paper I; Viti & Williams

1999) that the outflows can affect the chemical structure of the surrounding quiescent gas as a result of the interaction of photons generated in the associated shock structures with ice mantles on dust grains.

In this picture, the collimated outflow is driven by a jet, and the bow shock system at the head of the jet produces UV radiation. As a result of the associated radiation field, ice mantles are desorbed from the surfaces of dust particles. The ice mantles are mostly composed of simple saturated and stable species such as H_2O, CO and CH_4, and perhaps more complex species such as H_2CO and CH_3OH. This sudden enrichment of the gas-phase molecular abundances can drive a vigorous chemistry akin to that which is seen in molecular 'hot cores' (see, e.g., Walmsley & Schilke 1993). Thus, as well as the 'parent' saturated/stable species that are driven off the surface of grains, 'daughter' molecules, such as HCO^+, can be enhanced significantly by this process. In the case of HCO^+, the reaction sequence is initiated by the sublimation of mantle ices from the solid (s.) to the gas (g.) phase:

$$CO_{(s.)} \rightarrow CO_{(g.)},$$

$$H_2O_{(s.)} \rightarrow H_2O_{(g.)}.$$
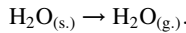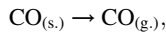
The CO can be photodissociated, and the C that is produced may then be photoionized:

$$CO + h\nu \rightarrow C + O,$$

$$C + h\nu \rightarrow C^+ + e^-.$$
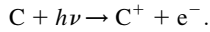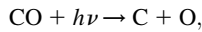
The subsequent reactions of C^+ with H_2O will enhance the HCO^+ abundance:

$$C^+ + H_2O \rightarrow HCO^+ + H. \tag{1}$$

Obviously, this enhancement can only be temporary, as the supply of excess C^+ and H_2O from evaporated mantles will be limited. Moreover, the H_2O is itself subject to photodissociation, whilst the HCO^+ is susceptible to dissociative recombination.

In the present work we propose that similar processes (though on a smaller spatial scale) to those occurring at the *head* of the jet also occur where the jet interacts with the dense protostellar core. The interaction with the clumpy core gas will be turbulent, and the interface is a location where mixing processes can generate significant chemical enhancements. We envisage that the jet sets up a range of high- and low-speed shocks in the core gas in the vicinity of the jet/core interface. High-speed shocks (~ 100 km s^{-1}) between the jet and the core gas generate an intense UV radiation field that can cause photodissociation and photoionization of molecules released from ices by sputtering in slower shocks (~ 30 km s^{-1}) that penetrate the denser ice-rich regions of the core. The estimated radiation field strength ($\sim 10 \times$ that in the ambient ISM; see below) may result in the grains being heated to ~ 25–35 K, but this will not be sufficient to evaporate the H_2O). Thus the proposal made here differs from that in Paper I. In the shock-free molecular cloud near the *head* of the jet, the liberation of ice mantles occurs as a result of the shock-generated radiation field, whereas in the situation *within the core*, shocks are constantly present and are assumed here to liberate the ice mantles directly from grains. Then, shock-generated UV radiation can promote the photochemistry that leads to enhanced HCO^+.

It should be stressed that the dynamics of turbulent interfaces between a fast wind and clumpy cold gas have not yet been properly evaluated. What is being suggested here is that the HCO^+ enhancement is a signature of that interface, and the

chemical model is evaluated for certain adopted radiation fields which are consistent with existing dynamical models of jet shock interfaces.

We define γ to be the enhancement factor for the HCO$^+$ abundance. That is to say, γ is the ratio of the HCO$^+$ abundance produced in the turbulent interface region in this model to the value obtained in a standard dark cloud chemical model. We now consider what values of γ are consistent with the HCO$^+$ emission from the turbulent interface region exceeding that from the bulk of the core. Our simplified model is depicted in Fig. 1(a), which shows a spherical core with a bipolar outflow surrounded by the interaction zone. This geometry can very roughly be approximated by a 'cored-apple' as in Fig. 1(b), where the jet has length R, width αR, and the interaction zone has thickness t. The ratio of the volume of the interaction zone to the total volume of the core is approximately

$$\frac{2\pi\alpha R \times 2R \times t}{\left(\frac{4}{3}\pi R^3\right)} = 3\alpha\left(\frac{t}{R}\right). \tag{2}$$

Thus, if the whole of the core is contained within the telescope beam, then HCO$^+$ emission from the interaction zone dominates if

$$3\alpha\left(\frac{t}{R}\right)\gamma > 1. \tag{3}$$

Now from our previous models (Paper I) we know that the thickness, t, of the interaction zone corresponds to around one magnitude of visual extinction, almost independent of density. For illustration, a core of mean hydrogen nucleon density
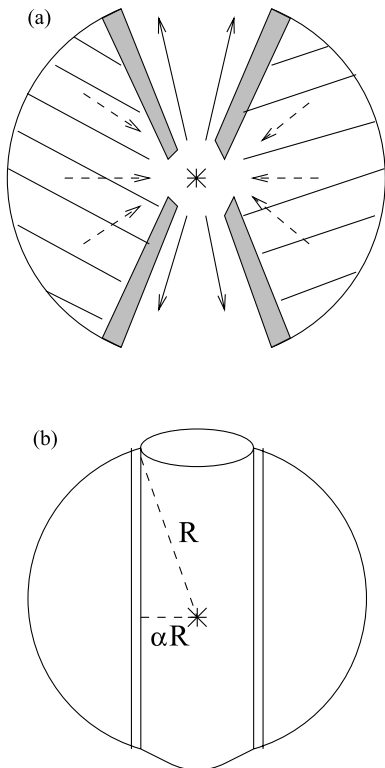

Figure 1. (a) Schematic of a cloud core that is undergoing collapse whilst simultaneously a bipolar outflow carries material away. The shaded area depicts the part of the envelope that is affected by the impinging shocks and the associated shock-generated radiation field. (b) Geometric representation of the interface surrounding the outflow.

$n_{\mathrm{H}} = 10^4\,\mathrm{cm}^{-3}$ and diameter $0.3\,\mathrm{pc}$ has a visual extinction through its centre of ~ 6 mag (assuming standard dust to gas ratios); hence $t/R \sim 0.17$. If $3\alpha \sim 1$ [corresponding to a jet opening angle of $2\sin^{-1}(1/3) \sim 39°$], then we require $\gamma \gtrsim 6$. We can estimate the HCO$^+$ abundance in a cold, quiescent core, simply by noting that in dark clouds HCO$^+$ is the dominant ion. Its fractional abundance, $x(\mathrm{HCO}^+)$, is therefore essentially the same order of magnitude as the total ionization fraction. Thus we can say

$$x(\mathrm{HCO}^+) \lesssim x(\mathrm{e}^-) \sim 10^{-8}\left(\frac{n_{\mathrm{H}}}{10^4\,\mathrm{cm}^{-3}}\right)^{-1/2} \tag{4}$$

(Hartquist & Williams 1989). For a density of $n_{\mathrm{H}} = 10^4\,\mathrm{cm}^{-3}$ we can see from (3) that the HCO$^+$ fractional abundance in the interaction zone must be $> 6 \times 10^{-8}$ to dominate over the HCO$^+$ in the quiescent gas. This is consistent with the observationally inferred abundance of $\sim 3.5 \times 10^{-8}$ in the inner core.

In order to ascertain the viability of the mechanism outlined above, we have employed a model that is similar to the one used in Paper I: the model describes the depth- and time-dependence of an interface region, which we characterize by a plane-parallel slab of gas (one-dimensional) that is illuminated on one side. The gas is at constant temperature and density ($10^4\,\mathrm{cm}^{-3}$), and the chemistry is followed as a function of both position (at 50 depth points) and time. The chemistry is the same as in Paper I, and is based on that used in Taylor, Morata & Williams (1996). It consists of a full reaction set (mainly drawn from the UMIST ratefile; Millar et al. 1991) for 145 gas-phase chemical species and 41 solid-state species which include the elements H, He, C, N, O, S and Mg. The elemental abundances are the same as those used in Table 1 of Paper I. There are 1480 gas-phase reactions and 99 freeze-out reactions; the accretion of C, N, O and S is assumed to be followed by a surface chemistry that leads to rapid hydrogenation, yielding CH$_4$, NH$_3$, H$_2$O and H$_2$S ices respectively. All other species are taken to be inert on the grain surface. No continuous desorption mechanisms are considered. All molecular ions that stick to grains are neutralized and subsequently retained in the ice mantles. H$^+$ is not adsorbed, and He$^+$, once neutralized, is returned to the gas phase. Any C$^+$ that is accreted is assumed to bond to the carbonaceous substrate, rather than being hydrogenated to form CH$_4$.

The initial conditions are found in a similar way to that described in Paper I; the chemistry is allowed to evolve, and molecular material to freeze-out on to the surface of dust grains (with a sticking efficiency of 0.3) for a period of 1 Myr. It is assumed that initially the gas is exposed to a weakened interstellar radiation field, which in units of the Draine (1978) radiation field is parametrized by the factor χ_0. In Paper I, a value of $\chi_0 = 0.3$ was adopted. In the current model we assume that the gas is exposed to a much lower UV flux, $\chi_0 = 0.03$, since it is part of a dense core. Although this parameter is somewhat arbitrary, it is found that the subsequent chemical evolution is not very sensitive to the value of χ_0. We have assumed that the extinction, A_v, is related to the hydrogen nucleon column density, N_{H}, by $N_{\mathrm{H}} = 1.6 \times 10^{21} A_v$, and that there is a uniform dust-to-gas ratio throughout the interface. The radiation field is attenuated at all positions accordingly, so that for most species the rates of the photoreactions are dependent on position alone. In the cases of H$_2$ and CO (which are both self-shielding) photodissociation rates are parametrically recalculated self-consistently as functions of both position and time in response to the changing column densities (following van Dishoeck & Black 1988).

Table 1. Fractional abundances at the end of the initial accretion phase, immediately before the ice mantles are desorbed and the shock-induced radiation field is turned on. The upper section gives the abundances at the (irradiated) edge of the slab, whilst the lower section gives the abundances at the innermost point in the model, corresponding to $A_v = 3.15$. The prefix 'g-' refers to solid-state species.

H	9.3(−1)	H$_2$	3.9(−2)	H$^+$	3.0(−6)	OH	2.2(−8)
O$_2$	1.3(−8)	H$_2$O	1.3(−9)	C	4.3(−13)	C$^+$	1.9(−11)
CH	1.2(−17)	CH$_4$	5.1(−18)	CO	1.1(−13)	HCO$^+$	6.8(−18)
H$_2$CO	1.3(−18)	HS	8.4(−21)	CS	2.2(−24)	SO	8.4(−19)
CO$_2$	7.6(−21)	NH	3.6(−12)	NH$_3$	2.9(−14)	HCN	1.8(−18)
N$_2$	5.6(−10)	NO	2.9(−9)	e$^-$	3.0(−6)	g-HNO	1.6(−12)
g-C	9.6(−5)	g-CO	1.5(−8)	g-H$_2$CO	5.6(−14)	g-C$_2$	1.5(−11)
g-CH	1.4(−11)	g-OH	1.6(−8)	g-NO	2.5(−9)	g-CH$_2$	2.8(−11)
g-H$_2$O	2.1(−4)	g-CO$_2$	3.9(−16)	g-CH$_3$	5.2(−11)	g-CH$_4$	1.0(−6)
g-HCO	2.1(−12)	g-N$_2$	7.4(−10)	g-CN	2.6(−12)	g-NH	3.0(−12)
g-HCN	2.3(−13)	g-C$_2$H	1.5(−12)	g-NH$_3$	3.8(−5)	g-N	7.0(−10)
g-O	7.7(−13)	g-O$_2$	9.3(−9)	g-NH$_2$	2.0(−12)	g-HS	9.4(−16)
g-CS	4.3(−14)	g-SO	8.6(−14)	g-H$_2$S	1.1(−10)	g-HCS	4.7(−16)
g-OCS	6.8(−19)	g-SO$_2$	1.3(−19)	g-S	1.2(−7)	g-NS	1.0(−16)
g-H$_2$CS	6.0(−17)	g-Mg	1.0(−7)	g-OCN	1.0(−16)	g-H$_2$CN	1.0(−16)
g-S$_2$	3.0(−20)	g-HS$_2$	5.2(−26)	g-O$_2$H	7.2(−20)	g-NO$_2$	2.4(−15)
H	4.5(−5)	H$_2$	5.0(−1)	H$^+$	9.0(−10)	OH	2.3(−8)
O$_2$	2.9(−6)	H$_2$O	9.5(−7)	C	2.0(−8)	C$^+$	1.6(−8)
CH	1.7(−10)	CH$_4$	4.1(−8)	CO	5.0(−5)	HCO$^+$	2.7(−9)
H$_2$CO	4.3(−9)	HS	7.8(−13)	CS	8.5(−10)	SO	2.5(−10)
CO$_2$	5.3(−9)	NH	6.5(−11)	NH$_3$	1.3(−8)	HCN	1.1(−9)
N$_2$	1.0(−5)	NO	8.2(−8)	e$^-$	2.8(−8)	g-HNO	6.9(−10)
g-C	3.4(−6)	g-CO	2.9(−5)	g-H$_2$CO	9.2(−9)	g-C$_2$	2.0(−9)
g-CH	2.8(−9)	g-OH	1.0(−8)	g-NO	2.4(−8)	g-CH$_2$	1.0(−9)
g-H$_2$O	1.7(−4)	g-CO$_2$	1.8(−9)	g-CH$_3$	2.5(−9)	g-CH$_4$	1.3(−5)
g-HCO	1.5(−8)	g-N$_2$	3.7(−6)	g-CN	5.9(−10)	g-NH	2.2(−11)
g-HCN	8.5(−9)	g-C$_2$H	8.7(−10)	g-NH$_3$	2.8(−5)	g-N	4.8(−10)
g-O	3.2(−13)	g-O$_2$	7.2(−7)	g-NH$_2$	1.1(−10)	g-HS	6.4(−12)
g-CS	7.6(−9)	g-SO	9.7(−11)	g-H$_2$S	9.3(−9)	g-HCS	4.6(−11)
g-OCS	4.7(−12)	g-SO$_2$	2.9(−12)	g-S	9.6(−8)	g-NS	2.5(−12)
g-H$_2$CS	5.6(−10)	g-Mg	1.0(−7)	g-OCN	2.3(−10)	g-H$_2$CN	3.6(−10)
g-S$_2$	1.7(−15)	g-HS$_2$	2.2(−15)	g-O$_2$H	2.0(−14)	g-NO$_2$	1.3(−11)

During this initial 'freeze-out' phase, the chemical composition of the interface varies between being primarily atomic (at the cloud edge) to molecular (at high extinctions). Consequently, there are significant chemical gradients, both in the gas phase, and in the mantle composition, across the slab. This is illustrated in Table 1, which gives the (final) gas-phase abundances (of selected species) and the solid-state abundances at the two extreme points in the slab: at the edge ($A_v = 0$), and at the deepest point in the interface (corresponding to $A_v = 3.15$). The abundance of C$^+$ is very much larger at $A_v = 3.15$ than it is at $A_v = 0$ (although the C$^+$:C ratio is larger at $A_v = 0$). This, rather counter-intuitive, result is a consequence of the Coulomb-enhanced freeze-out of C$^+$ (the most abundant carbon species at low A_v), which results in low gas-phase abundances for all carbon-bearing species at $A_v = 0$.

At $t = 0$ we turn on the radiation field (which we assume does not thereafter vary with time), and at the same time we assume that the ice mantles are shock-sputtered and returned instantaneously to the gas phase at all points in the interface simultaneously. Subsequent to mantle desorption, we follow the chemical evolution as functions of position and time throughout the interface. The density is taken to be constant at all positions in the interface. Compared to the physical conditions that were investigated in Paper I, the densities are higher, and the temperatures are higher due to the turbulent heating caused by the motion of the jet, but the shock velocities (and hence the strength of the radiation field) are expected to be lower.

In order to parameterize the radiation field, for the purpose of calculating the appropriate photorates, we follow the practice in Paper I and use the quantification by Wolfire & Königl (1991, 1993; see also Dopita & Sutherland 1995). These papers present comprehensive models of the radiation field and chemistry in Herbig–Haro objects associated with the heads of radiative stellar jets. The total emitted flux is $\propto n_0 v_s^3$, where n_0 is the pre-shock density, and v_s is the effective shock velocity (accounting for geometrical effects). For $v_s > 100\,\mathrm{km\,s^{-1}}$ the emergent flux is essentially described by a recombination spectrum. However, this is mostly in the form of line emission that does not overlap with the Lyman and Werner bands of H$_2$, nor the dissociation bands of CO. In addition to the line emission, there is a (relatively weak) far-ultraviolet continuum produced via He I and He II two-photon emission, which can dissociate H$_2$ and CO. In their standard model, Wolfire & Königl (1993) use $n_0 = 100\,\mathrm{cm^{-3}}$ (for the inter-clump medium) and $v_s = 200\,\mathrm{km\,s^{-1}}$, yielding total and continuum (capable of dissociating H$_2$ and CO) far-ultraviolet field strengths of $\chi_1 = 42\times$ and $\chi_c = 4.1\times$ the Habing field (Habing 1968) respectively. In Paper I we used $\chi_1 = 20$ and $\chi_c = 2$ in units of the Draine (1978) radiation field ($\sim 1.7\times$ the Habing field). The characteristics of the inner jet are enshrouded and essentially observable, so that there is no empirical indicator of either the pre-shock density or of the shock velocity in the interface region. However, we might expect the shock velocity to be less than $200\,\mathrm{km\,s^{-1}}$, and we therefore adopt a somewhat weaker radiation field than was used in Paper I: $\chi_1 = 10$ and $\chi_c = 1$. Although these values are somewhat arbitrary, they are certainly within the range
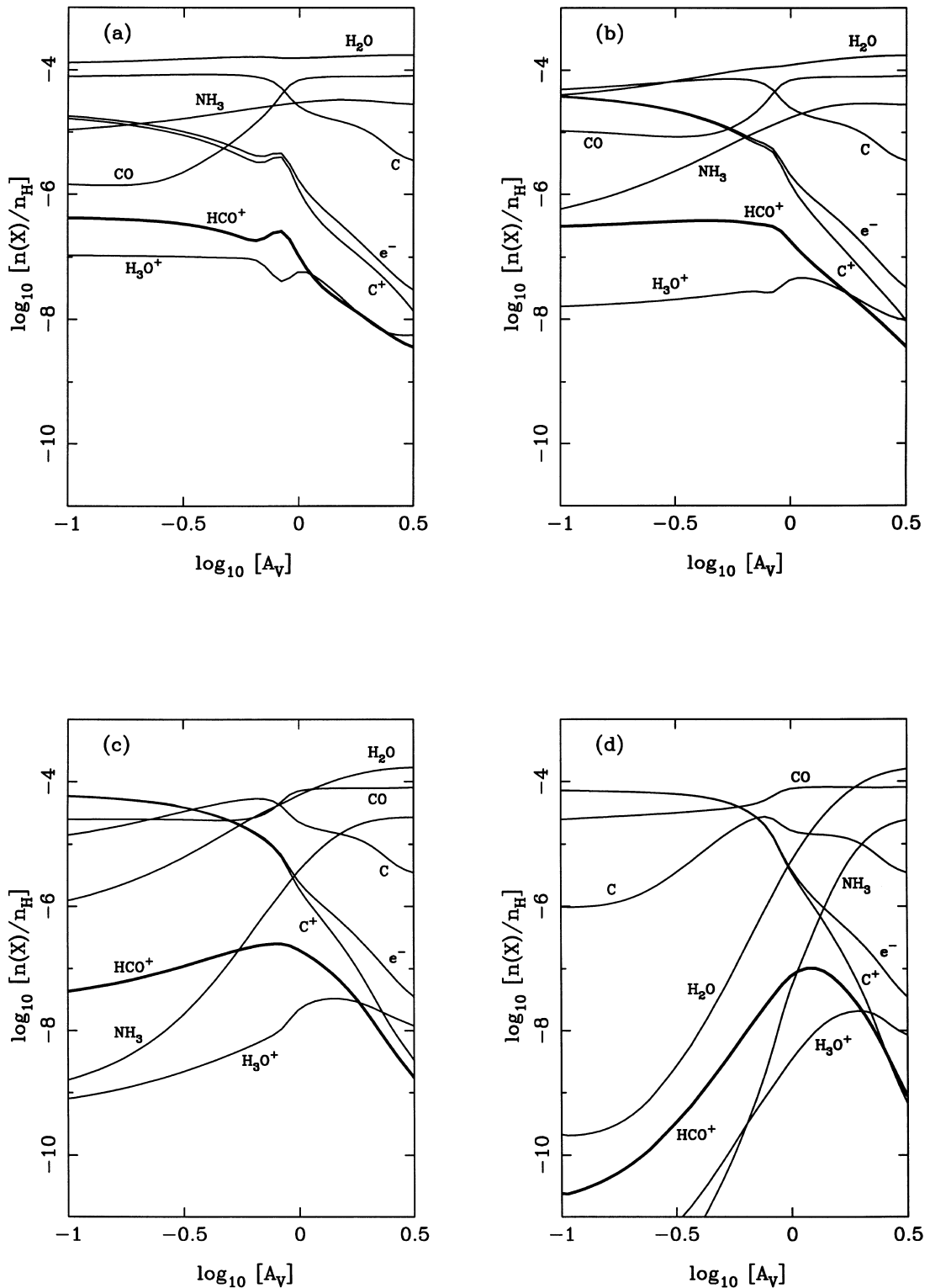
Figure 2. Fractional abundances (relative to hydrogen nuclei) of various species as a function of visual extinction (magnitudes) into the interface. The density and temperature of the clump material are $n_H = 10^4 \, \text{cm}^{-3}$ and $T = 100 \, \text{K}$. Results are given for various times after the ice mantles have been desorbed and the shock-induced radiation field has been turned on: (a) $t = 3 \, \text{yr}$, (b) $t = 10 \, \text{yr}$, (c) $t = 30 \, \text{yr}$, and (d) $t = 100 \, \text{yr}$.

expected from the models of Wolfire & Königl (1991, 1993) and Dopita & Sutherland (1995). In any case (see Section 3 below), our conclusions are not very sensitive to χ_1 and χ_c. In the next section we present results based on this assumed radiation field.

3   RESULTS

Our models show that the fractional abundances of HCO⁺, $x(\text{HCO}^+)$, can reach much higher values than those obtained in cold quiescent clouds. Moreover, the peak abundances greatly

exceed the values that were predicted for the less-attenuated gas that was the subject of Paper I. In Fig. 2 we show the fractional abundances of several selected species as a function of visual extinction from the shock edge. The (standard) parameters that we used for this run are $n_H = 10^4 \, cm^{-3}$, $T = 100 \, K$, $\chi_1 = 10$, and $\chi_c = 1$. Results are presented for several different times after the shock radiation is switched on: (a) 3 yr, (b) 10 yr, (c) 30 yr, and (d) 100 yr. The figures show how the zone of chemical enhancement 'eats' into the interface region as time progresses.

Providing the water abundance is not at saturation levels, the main loss route for HCO^+ is recombination:

$$HCO^+ + e^- \rightarrow CO + H, \qquad (5)$$

for which the rate coefficient possesses a steep inverse temperature dependence: $k = 3.3 \times 10^{-5}/T \, cm^3 \, s^{-1}$ (Smith & Adams 1984). For high H_2O fractional abundances the reaction

$$HCO^+ + H_2O \rightarrow H_3O^+ + CO, \qquad (6)$$
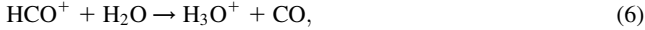
for which $k = 2.5 \times 10^{-9} \, cm^3 \, s^{-1}$ (Millar et al. 1991), becomes competitive. Recombination dominates over this reaction so long as

$$\frac{X(H_2O)}{X(e^-)} < 130 \quad [at \ 100 \, K]. \qquad (7)$$

From Fig. 2 it can be seen that at $A_v \gtrsim 1$ this inequality does not hold, and the upper limit to the (equilibrium) HCO^+ abundance will be obtained by balancing reaction (1) with reaction (6), yielding $x(HCO^+) \sim 0.36 \times x(C^+)$. This behaviour is apparent from Fig. 2 (especially for $t < 100 \, yr$), where the HCO^+ abundance clearly tracks the declining C^+ abundance at high extinctions.

The peak HCO^+ abundances in Fig. 2 range between 4.3×10^{-7} (at $t = 3 \, yr$) and 1.0×10^{-7} (at $t = 100 \, yr$), corresponding to abundance enhancements of $\gamma = 10$–43. These compare very favourably with the value of $\gamma \gtrsim 6$ that is necessary for the interface zone to dominate the HCO^+ emission and to account for the observed abundance excess. In practice, there will be a sheath of laterally entrained material between the jet and the chemically enhanced interface gas (see discussion), but it is clear that the interface region can, in principle, contribute far more to the total column density than the bulk of the surrounding quiescent gas. The total fractional abundances, γ-values, and implied column densities compare very well with the observed HCO^+ abundance enhancements, so we may conclude that our model is at least a viable mechanism for producing the high HCO^+ abundances that are inferred from observations.

In Fig. 3 we investigate the sensitivity of these results to the most significant free parameters: the radiation field strength and the density. Results are presented for a single snapshot in time at $t = 30 \, yr$. In Fig. 3(a) we show the effects of reducing the radiation field intensity. For this calculation, χ_1 and χ_c have been reduced to 5.0 and 0.5 respectively. We assume that (due to direct shock-driven mantle desorption) the desorption efficiency of CO and H_2O remains high. Quantitatively, the main effect of reducing the radiation field is that the HCO^+ abundance is enhanced by approximately 30–40 per cent. Qualitatively, there is more HCO^+ at low A_v, due to the increased survival time for H_2O. In Fig. 3(b) we show the results obtained for a higher core density: $n_H = 5 \times 10^4 \, cm^{-3}$. Here the differences are more strongly noticeable; the peak HCO^+ fractional abundances are severely reduced (by factors of between 0.045 and 0.13, for $t = 3$–100 yr). These
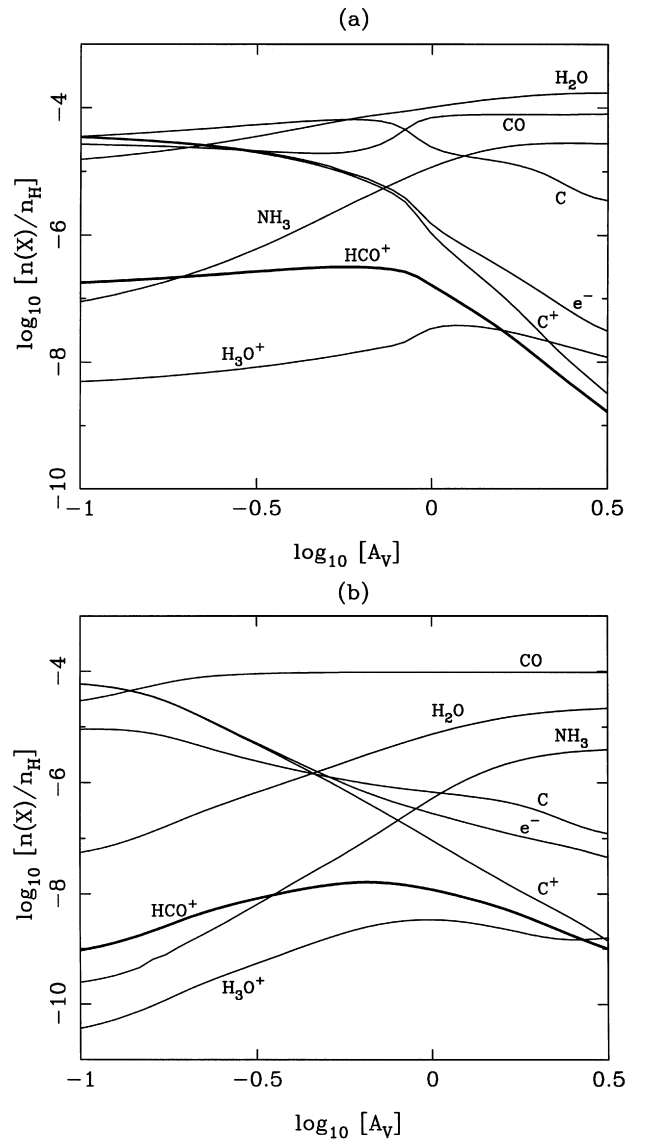

Figure 3. Fractional abundances (relative to hydrogen nuclei) of various species as a function of visual extinction (magnitudes) into the interface, at a time of $t = 30 \, yr$ after the ice mantles have been desorbed and the shock-induced radiation field has been turned on. (a) $\chi_1 = 5$, $\chi_c = 0.5$, (b) $n_H = 5 \times 10^4 \, cm^{-3}$. Other parameters are as for Fig. 2.

correspond to reductions in the number density of HCO^+ by factors of between 0.22 and 0.65. In addition, the abundance peaks occur at somewhat lower values of A_v. Nevertheless, the abundance enhancements at early times ($\gamma \sim 5$–10 for $t < 100 \, yr$) are still sufficient to be able to explain the observed abundance anomaly.

The gas temperature may be higher than the value that we have adopted (100 K); significant photoelectric heating may result from the shock-generated UV radiation field. We have therefore performed calculations at a somewhat higher temperature (150 K). The results are qualitatively very similar, although, as expected, higher HCO^+ abundances can be produced due to the inverse temperature dependence of the rate-coefficient for HCO^+ recombination (reaction 5). Enhancements of the peak HCO^+ abundances by 35–40 per cent are produced.

4 DISCUSSION

Although our results lend support to the idea that the gas–grain chemistry can be boosted in an irradiated shock interface region to a degree that is consistent with the observed overabundance of HCO$^+$ in protostellar cores, we acknowledge that some major simplifications have been made. First, the abundances that have been inferred from the observations, and which we have attempted to model, have been deduced on the assumption of a specific dynamical scenario (spherically symmetric, inside-out collapse) that is very different to the 2D axisymmetric geometry that forms the basis of our model. The dynamical aspects of the outflow and interface are beyond the scope of this paper, and whether or not the jet/interface geometry will yield similar asymmetric self-reversed line profile shapes is not at all clear. On the other hand, it must be recognized that there is considerable ambiguity in the interpretation of the line profiles in any case – they are consistent with, but not conclusive proof of, the spherically symmetric infall model. Secondly, throughout our discussions we have simply been concerned with the HCO$^+$ abundance. In the observational context, careful attention should be paid to the excitation of HCO$^+$. However, the HCO$^+$ excitation should be nearly the same as in the quiescent gas, since the density is barely changed by the mantle desorption and photolysis effects that are the basis of our model. Moreover, the collisional rate coefficients for the excitation of HCO$^+$ by H$_2$ impact do not have a strong temperature dependence (Monteiro 1985).

A potentially more serious flaw concerns the global effects that may occur to the chemistry. As we remark in Section 2 above, the mechanism that we have invoked bears some similarity to the 'hot-core' chemistry that pertains in the vicinity of ultracompact H II regions within molecular cores. However, as with the hot-core chemistry, the chemical effects of sudden mantle desorption and strong irradiation are not limited to a single species. Thus the mechanism that causes the HCO$^+$ abundance anomalies should also result in (not necessarily similar) abundance anomalies in other molecular species, such as NH$_3$, CO$_2$, CH$_3$OH and H$_2$CO. Typically, the abundances of these species are enhanced due to surface processes. Unfortunately, there are very few reliable abundance measurements for B335; Menten et al. (1984) found that $X(NH_3) \lesssim 2 \times 10^{-9}$, whilst recent line surveys (Evans & Rawlings, unpublished data) suggest that in the infall region $X(N_2H^+) \sim 3.2 \times 10^{-9}$ and $X(H_2CO) \sim 4.1 \times 10^{-9}$. Comparing to the results from our model, it is immediately apparent that the observed NH$_3$ abundance is very much less than the model predictions *at early times*, but the qualitative development of the NH$_3$ with time is very different to that of the HCO$^+$, whose enhancement is driven by the secondary mechanism described in Section 2. The NH$_3$ enhancement results from primary desorption from the grain mantles, and is therefore more transitory; by $t = 30$ yr (Fig. 2c), the NH$_3$ abundance at the edge of the interface has dropped to $< 2 \times 10^{-9}$, whilst the HCO$^+$ abundance is still strongly enhanced. Deeper into the cloud the higher abundances of NH$_3$ may be an artefact of our assumption concerning the mantle desorption efficiency at large depths into the interface.

The success, or otherwise, of this model as an explanation of the HCO$^+$ abundance anomaly in infall sources largely depends on whether or not the effects can be sustained over a long period of time. As with any chemistry that depends on the sudden injection of material into the gas phase from ice mantles, the chemical enhancements are inevitably transient and, depending on the densities and temperatures in the clouds, may only be short-lived.

This applies to the hot-core chemistries as well as to the irradiated clump chemistry that was investigated in Paper I. From Fig. 2 it can be seen that the HCO$^+$ abundance peak 'eats into' the interface region on a time-scale of some 30–100 yr. Obviously, if the interface were fixed in space, then this time-scale would be far too short for the mechanism to be viable. However, we should not treat the interface as being static. Rather, as can be deduced from the time dependence of the HCO$^+$ abundance profiles in Fig. 2, the region of chemical enrichment will start in the immediate vicinity of the outflow, and will steadily progress deeper into the surrounding molecular core. This chemical enhancement wave could then take many thousands of years to spread through the surrounding molecular core. It is well known that the youngest protostellar sources generate the most highly collimated jets, and recent interferometric observations of the embedded IRS1 protostellar core in B5 have provided direct evidence in support of our physical picture (Velusamy & Langer 1998). The outflow cones of this source, as seen in ^{12}CO(2–1), are very wide (with an opening angle in excess of 90°) and have a parabolic shape, suggesting that the opening angle is growing at a rate of $0°.006 \, yr^{-1}$. We note that this growth rate is very similar to the time-scale for the propagation of the chemical enhancement wave that we have described in this paper. Support for our model is also provided in a recent survey of young low-mass star-forming regions in HCO$^+(J = 1 \rightarrow 0)$ by Hogerheijde et al. (1998). Their high-resolution observations with the Owens Valley Millimetre Array of L1527, which is a well-defined outflow source (with an outflow length of ~ 0.12 pc) show a clearly defined 'butterfly' morphology with an opening angle of $\sim 90°$ (Fig. 1). This distribution is interpreted as originating from enhanced HCO$^+$ emission associated with the walls of the outflow cavity. Their observations suggest that the HCO$^+$ is enhanced by a factor of $\sim 10\times$ in these regions, and that the fractional abundance of HCO$^+$ in their sources is $\sim 4 \times 10^{-8}$ on the length-scales sampled by the interferometer. Both the observations and the interpretation are consistent with the model that we have proposed.

Obviously, a fully descriptive model of the chemistry would involve a transformation into the rest frame of the interface. We would then have to include an advection term describing the transport of fresh material into the radiation-dominated zone. However, we do not have a clear picture of the physical nature of the advection term, which may derive from a turbulent ablation process. Hence such a sophisticated modelling approach cannot be justified. Rather, we adopt a semi-empirical approach; in the context of this argument it is essential to realize that (unlike NH$_3$) the HCO$^+$ column density does not vary significantly with time: From Fig. 2, $N(HCO^+) = 4.83$, 6.35 and 4.06×10^{14} cm^{-2}, whilst $N(NH_3) = 1.38$, 1.02 and 0.68×10^{17} cm^{-2} at $t = 3$, 10 and 30 d respectively. Thus we have obtained a positive result by noting that the only physical parameter that we can approximately quantify, the time-scale for the progression of the interface into the clump, is comparable to that for the progression of the HCO$^+$ enhancement peak.

As was discussed in Paper I, it is also possible that our chemical model may be underestimating the HCO$^+$ formation efficiency; the main product of reaction (1) is in fact HOC$^+$ and not HCO$^+$, but if effective conversion can take place through reaction with H$_2$, then the net HCO$^+$ formation efficiency may be higher. Also, if CO is hydrogenated on the surface of grains to H$_2$CO or CH$_3$OH, then the subsequent photoprocessing of these molecules, once desorbed from the grains, could yield more HCO$^+$. Finally, we note that a further source of HCO$^+$ may be the interface

between the jet and core gas where material can be laterally entrained and a chemistry take place. Taylor & Raga (1995) showed that HCO^+ can be much enhanced in this layer. In models of diffusive interfaces between hot (10^4 K) winds and dense, cool clump material ($n_H = 5 \times 10^4$ cm^{-3}, $T = 10$ K), Rawlings & Hartquist (1997) described the chemistry in an interface region with similar thickness (equivalent to ~ 0.7 magnitudes of extinction) to the interfaces described in this paper. They found that diffusive mixing alone could lead to HCO^+ abundance enhancements of up to three orders of magnitude. The maximum HCO^+ column density that is obtained (Table 3) is 3.5×10^{12} cm^{-2}, corresponding to an average HCO^+ abundance of 5×10^{-9}. This is somewhat too small to account for the observations, but these calculations only describe diffusion, and do not include the effects of any gas–grain interactions.

ACKNOWLEDGMENTS

REFERENCES

Bachiller R. et al., 1995, A&A, 299, 857
Choi M., Evans N. J. II, Gregersen E. M., Wang Y., 1995, ApJ, 448, 742
Dalgarno A., Lepp S., 1984, ApJ, 287, L47
Dopita M. A., Sutherland R. S., 1995, ApJ, 455, 468
Draine B. T., 1978, ApJS, 36, 595
Gregersen E. M., Evans N. J., II, Zhou S., Choi M., 1997, ApJ, 484, 256
Habing H. J., 1968, Bull. Astron. Inst. Netherlands, 19, 421
Hartquist T. W., Williams D. A., 1989, MNRAS, 241, 417
Hogerheijde M. R., van Dishoeck E. F., Blake G. A., van Langevelde H. J., 1998, ApJ, 502, 315
Menten K. M., Walmsley C. M., Krugel E., Ungerechts H., 1984, A&A, 137, 108
Millar T. J., Rawlings J. M. C., Bennett A., Brown P. D., Charnley S. B., 1991, A&AS, 87, 585
Monteiro T., 1985, MNRAS, 214, 419
Rawlings J. M. C., 1996, QJRAS, 37, 503
Rawlings J. M. C., Hartquist T. W., 1997, ApJ, 487, 672
Rawlings J. M. C., Hartquist T. W., Menten K. M., Williams D. A., 1992, MNRAS, 255, 471
Rawlings J. M. C., Evans N. J., II, Zhou S., 1993, Ap&SS, 216, 155
Shu F. H., 1977, ApJ, 214, 488
Smith D., Adams N. G., 1984, ApJ, 284, L13
Taylor S. D., Morata O., Williams D. A., 1996, A&A, 313, 269
Taylor S. D., Raga A. C., 1995, A&A, 296, 823
Taylor S. D., Williams D. A., 1996, MNRAS, 282, 1343 (Paper I)
van Dishoeck E. F., 1998, in Hartquist T. W., Williams D. A., eds, The Molecular Astrophysics of Stars and Galaxies. Clarendon Press, Oxford, p. 53
van Dishoeck E. F., Black J. H., 1988, ApJ, 334, 771
Velusamy T., Langer W. D., 1998, Nat, 392, 685
Viti S., Williams D. A., 1999, MNRAS, 310, 517
Walker C. K., Lada C. J., Young E. T., Maloney P. R., Wilking B. A., 1986, ApJ, 309, L47
Walmsley C. M., Schilke P., 1993, in Millar T. J., Williams D. A., eds, Dust and Chemistry in Astronomy. Institute of Physics Publishing, Bristol, p. 37
Williams J. P., Bergin E. A., Caselli P., Myers P. C., Plume R., 1998, ApJ, 503, 689
Wolfire M. G., König A., 1991, ApJ, 383, 205
Wolfire M. G., König A., 1993, ApJ, 415, 204
Zhou S., Evans N. J. II, Kömpe C., Walmsley C. M., 1993, ApJ, 404, 232
Zhou S., Evans N. J., II, Wang Y., Peng R., Lo K. Y., 1994, ApJ, 433, 131

This paper has been typeset from a TEX/LATEX file prepared by the author.